J|A|C|S
ARTICLES
Published on Web 12/28/2001

# Carboxylates Stacked over Aromatic Rings Promote Salt Bridge Formation in Water

Samuel E. Thompson and David B. Smithrud*

*Contribution from the Department of Chemistry, University of Cincinnati, Cincinnati, Ohio 45221-0172*

Received August 14, 2001

***Abstract:*** Several salt bridges observed in protein X-ray crystallographic structures showed a consistent pattern of a carboxylate, situated near the face of an aromatic ring, forming a bond to an arginine residue of a ligand. To determine the driving force for these complexes, $^1$H NMR or potentiometric binding titrations were performed on solutions containing *N*-acetyl arginine methyl ester, *N*-acetyl lysine methyl ester, guanidinium chloride, or KCl and one member of a series of diacidic templates, which had aromatic or aliphatic groups placed below their carboxylates. Only templates having an aromatic ring were able to form a salt bridge in water. Although most of the obvious interactions, such as ionic and cation$-\pi$, and ion desolvation are important factors, association of an amino acid in water required the presence of the entire amino acid. This result suggests that the interaction between the aliphatic portion of an amino acid and an aromatic ring of a template is an important component of complexation. Aromatic templates also transported *N*-acetyl arginine methyl ester from water to 1-octanol. The results of the transport studies are discussed in terms of potential intermediate states that could lower some of the activation barriers of protein folding.

## Introduction

Charged amino acids are found throughout proteins, with a greater percentage existing in solvent-exposed regions. At first glance, it may seem natural for these functional groups to form salt bridges with complementary charged amino acids to provide protein stability and ligand binding. However, unlike the hydrophobic effect that provides the driving force for protein folding[1] and a large portion of the binding energy for protein complexes, the energy contributed to these processes by salt bridges is deemed either favorable,[2] approximately none,[3] or unfavorable,[4] depending on the experiment, calculation, or computational analysis. The contradictory nature of salt bridges arises from the opposing energy terms in water, the pairwise Coulombic interaction energy being favorable, whereas ion desolvation is an unfavorable process. The magnitude of these energy terms depends on many factors, including the size of the charge and the dielectric constant of the media that surround the isolated ions and the complex.[2−4] Although a large desolvation penalty generally leads to unfavorable salt bridge formation, the extreme case of burying a salt bridge within the hydrophobic core of a protein with almost complete desolvation of the ion pair may still be energetically favorable.[5]

Even though early calculations showed that approximately 10−16 kcal/mol of energy is lost upon transfer of a salt bridge from water to a protein interior,[6] salt bridges seem to be an important bond for protein folding and structure. Protein folding results from an accumulation of small favorable energy terms, and thus, even weak ionic bonds may contribute to protein structure and function. One classic example is the allosteric transition of hemoglobin. Salt bridges are postulated to stabilize the T state of the protein, and once broken, the protein reverts to its R state.[7] Recent studies on the constituents of hyperthermal proteins have shown that they contain a greater number of salt bridges compared to mesophilic ones.[8] Deletion of salt bridges can lead to destabilized proteins,[9] and the addition of salt bridges at the $i$ and $i + 4$ positions in short peptides[10] or on protein surfaces[11] can promote the formation of α-helices. Consistent with the confusing nature of salt bridges, for all the cases of favorable salt bridges there seems to be an equal number of

* To whom correspondence should be addressed. Tel.: (513) 556−9254. Fax: (513) 556−9239. E-mail david.smithrud@uc.edu.

(1) Dill K. A. *Biochemistry* **1990**, *29*, 7133−7155.
(2) (a) Lounnas, V.; Wade, R. C. *Biochemistry* **1997**, *36*, 5402−5417. (b) Xu, D.; Lin, S. L.; Nussinov, R. *J. Mol. Biol.* **1997**, *265*, 68−84. (c) Pervushin, K.; Billeter, M.; Siegal, G.; Wuthrich, K. *J. Mol. Biol.* **1996**, *264*, 1002−1012. (d) Marqusee, S.; Sauer, R. T. *Protein Sci.* **1994**, *3*, 2217−2225. (e) Horovitz, A.; Fersht, A. R. *J. Mol. Biol.* **1992**, *224*, 733−740.
(3) (a) Barril, X.; Aleman, C.; Orozco, M.; Luque, F. J. *Proteins: Struct., Funct. Genet.* **1998**, *32*, 67−79. (b) Serrano, L.; Horovitz, A.; Avron, B.; Bycroft, M.; Fersht, A. R. *Biochemistry* **1990**, *29*, 9343−9352. (c) Singh, U. C. *Proc. Natl Acad. Sci. U.S.A.* **1988**, *85*, 4280−4284.
(4) (a) Waldburger, C. D.; Jonsson, T.; Sauer, R. T. *Proc. Natl Acad. Sci. U.S.A.* **1996**, *93*, 2629−2634. (b) Hendsch, Z. S.; Tidor, B. *Protein Sci.* **1994**, *3*, 211−226. (c) Sun, D. P.; Sauer, U.; Nicholson, H.; Matthews, B. W. *Biochemistry* **1991**, *30*, 7142−7153.
(5) Kumar, S.; Nussinov, R. *J. Mol. Biol.* **1999**, *293*, 1241−1255.
(6) Honig, B. H.; Hubbell, W. L. *Proc. Natl. Acad. Sci. U.S.A.* **1984**, *81*, 5412−5416.
(7) Perutz, M. F. *Q. Rev. Biophys.* **1989**, *22*, 139−237.
(8) (a) Aguilar, C. F.; Sanderson, I.; Moracci, M.; Ciaramella, M.; Nucci, R.; Rossi, M.; Pearl, L. H. *J. Mol. Biol.* **1997**, *271*, 789−802. (b) Russell, R. J. M.; Ferguson, J. M. C.; Hough, D. W.; Danson, M. J.; Taylor, G. L. *Biochemistry* **1997**, *36*, 9983−9994. (c) Lim, J. H.; Yu, Y. G.; Han, Y. S.; Cho, S. J.; Ahn, B. Y.; Kim, S. H.; Cho, Y. J. *J. Mol. Biol.* **1997**, *270*, 259−274.
(9) Kawamura, S.; Tanaka, I.; Yamasaki, N.; Kimura, M. *J. Biochem.* **1997**, *121*, 448−455.
(10) Huyghues-Despointes, B. M. P.; Baldwin, R. L. *Biochemistry* **1997**, *36*, 1965−1970.
(11) Serrano, L.; Horovitz, A.; Avron, B.; Bycroft, M.; Fersht, A. R. *Biochemistry* **1990**, *29*, 9343−9352.


**10.1021/ja011973h CCC: $22.00** 

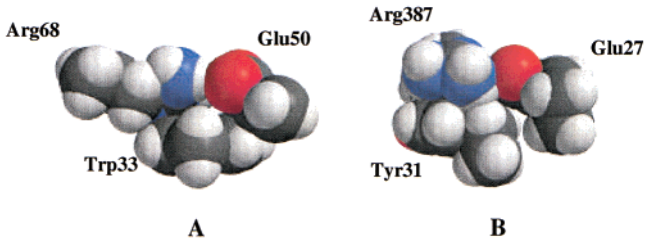


***Figure 1.*** Representative SACA structures found (A) at the protein binding interface of lysozyme and the antibody HyHEL-5[19] and (B) within the α-amylase protein.[2b] The aromatic rings of Trp33 and Tyr31 activate the carboxylates of glu50 and glu27, respectively, making salt bridge formation a more favorable process in water.

unfavorable ones. Replacing salt bridges within a variant of Arc repressor with hydrophobic residues increased protein stability,[12] and energy estimates of some buried salt bridges using continuum electrostatic calculations[5] are unfavorable. Incorporating salt bridges within proteins definitely does not guarantee a favorable energy term. The addition of a salt bridge into an α-helix dimer destabilized it,[13] and a salt bridge incorporated into a surface helix of T4 lysozyme appeared to have little effect on protein stability.[14]

Our interest in the properties of salt bridges derives from our desire to create simple biomimics of protein binding domains that exist in antibodies and receptors. Considering the uncertain energetic nature of salt bridges, creating compounds that contain amino acids with hydrophobic side chains might seem to be a more reasonable choice. However, a true mimic of an antibody or receptor needs to exist as a monomer in an aqueous environment until it contacts its binding partner. Additionally, salt bridges may play an important role in ligand binding, because the same forces used for protein folding are available and the desolvation penalty is smaller.[2b] The formation and dissolution of salt bridges appears to be one mechanism that receptors use to propagate signals across membranes.[15,16] Salt bridge formation seems to be an important component in the binding of integrins to the RGD universal recognition sequence.[17] Ionic bonds are also necessary in some antigen−antibody complexes, such as in the complex of HyHEL-10[18] and HyHEL-5[19] with lysozyme.

HyHEL-5 binds lysozyme strongly with an association constant of $2.5 \times 10^9$, and one epitope has Arg68 of lysozyme associated with the side chains of Glu50, Asn58, and Trp33 held in a stacked arrangement on HyHEL-5's surface (Asn58 might not interact with Arg68[19b]) (Figure 1A). Arg68 is a key residue for complexation. Having Lys in its position reduces the affinity of the antibody for lysozyme by a factor of $10^3$.[19b,20] We wanted to determine if this stacked arrangement of side chains, which we call SACA (*s*tacked *a*rrangement of *c*arboxylates over *a*romatic rings), occurs by happenstance or if this arrangement provides for an energetic advantage. A cursory examination of a disparate group of protein complexes resulted in the identification of other potential SACA sites, and these sites are all associated with an arginine residue of their ligand. In the complex between the human growth hormone receptor ($hGH_R$) and the human growth hormone (hGH), Glu44, Asp164, and Trp169 are on the surface of $hGH_R$ and interact with Arg64 of hGH.[21,22] Because these three residues provide the majority of the binding energy for the complex, they are referred to as a "hot spot". A potential SACA site is also found in the binding of fibrinogen to the tripeptide Gly-Pro-Arg.[23] Arg3 of the tripeptide is positioned between the phenol ring of Tyr363 and the two carboxylates of Asp330 and Asp364. SACA sites are not reserved for protein surfaces. A potential site was found buried in the human salivary α-amylase protein (Figure 1B).[2b]

These binding sites reveal a salt bridge between an arginine residue and at least one carboxylate in the presence of an aromatic ring. The role of the ions is obvious, but what role does the aromatic ring serve in salt bridge formation? It has been long known that arginines are generally found to be associated with aromatic rings in proteins. Fifty percent of arginines are within van der Waals contact distance.[24] The combination of the cation−$\pi$ interaction[25] and van der Waals forces is believed to align arginine's side chain for the binding to ligands or to other side chains to maintain protein structure.[24−26] We wanted to test these assumptions and further propose that the position of the aromatic ring also activates the carboxylate (anion−$\pi$ interactions), making salt bridge formation a more favorable process in water. Templates **1**−**4** and Boc-Phe-Asp-Asp were constructed, and their properties were investigated to determine whether, and if so how, the presence of an aromatic ring enhances the formation of salt bridges between their carboxylates and *N*-acetyl-L-arginine methyl ester (Arg(**I**)) or *N*-acetyl-L-lysine methyl ester (Lys(**II**)) in DMSO and water. We hope to show that the SACA structure is a strong candidate for a protein-binding motif and that SACA templates are promising lead compounds for the creation of novel compounds that bind positively charged side chains exposed on protein surfaces.

## Results

To determine whether a SACA structure is necessary for binding positively charged amino acids in water, the properties of templates **1** and **2**, whose aromatic rings mimic tyrosine and phenylalanine, respectively, were compared to those of templates **3** and **4**, which do not contain an aromatic surface (Chart 1). The association constants of the templates bound to both Arg(**I**) and Lys(**II**) are more strongly affected by the presence of an aromatic ring in water than in DMSO (Table 1). In DMSO-$d_6$, substantial shifts in the resonances of α-H and $\delta$-H protons for Arg(**I**) and α-H and $\epsilon$-H protons for Lys(**II**) were observed

(12) Hendsch, Z. S.; Jonsson, T.; Sauer, R. T.; Tidor, B. *Biochemistry* **1996**, *35*, 7621−7625.
(13) Schneider, J. P.; Lear, J. D.; DeGrado, W. F. *J. Am. Chem. Soc.* **1997**, *119*, 5742−5743.
(14) Daopin, S.; Sauer, U.; Nicholson, H.; Matthews, B. W. *Biochemistry* **1991**, *30*, 7142−7153.
(15) Zhorov, B. S.; Ananthanarayanan, V. S. *Arch. Biochem. Biophys.* **2000**, *375*, 31−49.
(16) Porter, J. E.; Perez, D. M. *J. Pharm. Exp. Ther.* **2000**, *292*, 440−448.
(17) Baneres, J. L.; Roquet, F.; Martin, A.; Parello, J. *J. Biol. Chem.* **2000**, *275*, 5888−5903.
(18) (a) Pons, J.; Rajpal, A.; Kirsch, J. F. *Protein Sci.* **1999**, *8*, 958−968. (b) Padlan, E. A.; Silverton, E. W.; Sheriff, S.; Cohen, G. H.; Smith-Gill, S. J.; Davies, D. R. *Proc. Natl. Acad. Sci. U.S.A.* **1989**, *86*, 5938−5942.
(19) (a) Cohen, G. H.; Sheriff, S.; Davies, D. R. *Acta Crystallogr.* **1996**, *D52*, 315−326. (b) Sheriff, S.; Silverton, E. W.; Padlan, E. A.; Cohen, G. H.; Smith-Gill, S. J.; Finzel, B. C.; Davies, D. R. *Proc. Natl. Acad. Sci. U.S.A.* **1987**, *84*, 8075−8079.
(20) Smith-Gill, S. J.; Wilson, A. C.; Potter, M.; Prager, E. M.; Feldmann, R. J.; Mainhart, C. R. *J. Immunol.* **1982**, *128*, 314−322.
(21) Somers, W.; Ultsch, M.; de Vos, A. M.; Kossiakoff, A. A. *Nature* **1994**, *372*, 478−481.
(22) Clackson, T.; Ultsch, M. H.; Wells, J. A.; de Vos, A. M. *J. Mol. Biol.* **1998**, *277*, 1111−1128.
(23) Spraggon, G.; Everse, S. J.; Doolittle, R. F. *Nature* **1997**, *389*, 455−462.
(24) Burley, S. K.; Petsko, G. A. *FEBS Lett.* **1986**, *203*, 139−143.
(25) Ma, J. C.; Dougherty, D. A. *Chem. Rev.* **1997**, *97*, 1303−1324.
(26) Bullesbach, E. E.; Schwabe, C. *J. Biol. Chem.* **2000**, *275*, 35276−35280.

***Chart 1.*** Structures for the SACA Templates and the Derivatized Amino Acids

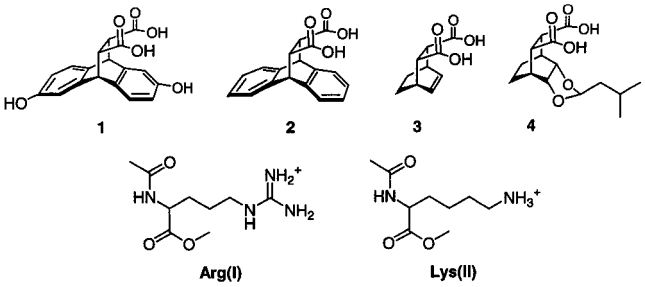


***Table 1.*** Free Energy of Binding between Templates and the Amino Acid Derivatives at 298 K

| | | ΔG° (kcal/mol) | |
|---|---|---|---|
| compound | solvent | arginine I | lysine II |
| **1** | water[a] | −1.2[b] | −1.5 |
| | DMSO-$d_6$[c] | −2.3 | −4.0 |
| **2** | water | −1.1 | −1.0 |
| | DMSO-$d_6$ | −2.4 | −3.5 |
| **3** | water | n.b.[d] | n.b. |
| | DMSO-$d_6$ | −2.6 | −4.2 |
| **4** | water | n.b. | n.b. |
| | DMSO-$d_6$ | −1.8 | > −4 |
| Boc-Phe-Asp-Asp | water | n.b. | n.b. |
| | DMSO-$d_6$ | −3.3 | > −4 |

[a] 90/10, pH 7.5 sodium phosphate (50 mM) $D_2O$. [b] Uncertainties in the free energies are ±0.1 kcal/mol. [c] Counterions were $N(Et)_4^+$. [d] n.b., no binding was detected.

when the concentration of the templates **1**−**4** or Boc-Phe-Asp-Asp was increased. In the converse experiment, smaller changes in the chemical shifts of the template's protons were observed upon increasing the concentration of the amino acid and holding the concentration of the template constant. We also observed changes in the UV−vis spectrum of templates **1** and **2** with changes in the concentration of the amino acids in DMSO. In the case of template **2** binding Lys(**II**), an isosbestic point existed in the titration plot (data not shown), indicating that only a single equilibrium mixture existed in the assay. At higher concentrations of the amino acid, the absorbance curve did not pass through the isosbestic point, which indicates that a second complex was formed. Most likely the new species is a trimer formed between two Lys(**II**)'s and one template **2**. Evidence for the existence of higher ordered complexes in DMSO-$d_6$ was also obtained in the $^1$H NMR titrations. At higher concentrations of the binding partners, new peaks appeared that shifted with changes in concentration. To avoid these complications in deriving accurate association constants, the concentrations of the binding components in the assays were kept below the level that produced a detectable amount of higher ordered complexes.

In the various aqueous solutions, significant shifts in proton resonances occurred for Lys(**II**) and Arg(**I**) in the presence of templates **1** and **2** but not in the presence of templates **3** and **4** or Boc-Phe-Asp-Asp. Using Arg(**I**) as an example, no shifts in resonances were observed for the protons of Arg(**I**) (50 mM) until the concentration of template **3** reached 100 mM ($\Delta\delta$ < 0.01 ppm), and no shifts were observed for template **4** at this concentration. The chemical shifts of the Arg(**I**) protons remained constant at higher concentrations of template **3**. In contrast, changes in the chemical shift of the $\delta$-H proton of Arg(**I**) (25 mM) were observed in the presence of 5 mM template **1** ($\Delta\delta$ = 0.01 ppm), and this value continued to increase with increasing concentration of template **1** ($\Delta\delta$ = 0.34 ppm at [**1**] = 150 mM). Similar results were obtained for template **2**. No association was observed between template **1** and Arg(**I**) when the $^1$H NMR titrations were performed at pH 3.0, which suggests that a salt bridge is necessary for association. Hydrophobic groups were also necessary since simple ions form weak salt bridges in water.[27] No changes were observed in the $^1$H NMR spectrum of solutions containing Lys(**II**) (40 mM) or Arg(**I**) (40 mM) and potassium acetate (0.4 M). The same association constants were obtained for templates existing as disodium salts in $D_2O$ with or without the presence of 0.1 M potassium phosphate (pH 7.5). Thus, phosphate buffers did not have an effect on binding.

***Table 2.*** Changes in p$K_a$'s and Free Energy Values for Diacids at 298 K as Determined by Potentiometric Titrations

| compound | condition | p$K_{a2}$[a] | $\Delta G^{\circ}$[b] (kcal/mol) |
|---|---|---|---|
| **1** | neat[c] | 6.1 | |
| | 1 M KCl | 5.3 | −0.9 |
| | 1 M $GH^+$ | 5.3 | −0.9 |
| | 0.05 M Arg(**I**) | 5.1 | −3.1 |
| **2** | neat | 6.4 | |
| | 1 M KCl | 5.4 | −1.3 |
| | 1 M $GH^+$ | 5.3 | −1.6 |
| | 0.05 M Arg(**I**) | 5.7 | −2.6 |
| **3** | neat | 6.6 | |
| | 1 M KCl | 5.7 | −1.2 |
| | 1 M $GH^+$ | 5.5 | −1.5 |
| | 0.05 M Arg(**I**) | 6.5 | −1.2 |
| **4** | neat | 5.2 | |
| | 1 M KCl | 4.9 | 0.1 |
| | 1 M $GH^+$ | 4.6 | −0.6 |
| | 0.05 M Arg(**I**) | 5.1 | −0.8 |

[a] Standard deviations are ±0.1. [b] Free energy values are calculated from $\Delta pK_{a2}$ values and by assuming the drops in p$K_a$ result from binding. [c] Neat conditions refer to titrations performed without additional salts added. These values were within experimental errors of values obtained in 0.1 M KCl solutions.

To test whether the position of an aromatic ring relative to the carboxylate is important for association, we studied the properties of Boc-Phe-Asp-Asp. No changes in chemical shifts were observed ($\Delta\delta$ < 0.005 ppm) for aqueous solutions (90/10 0.1 M phosphate buffer pH 7.5/$D_2O$) of Boc-Phe-Asp-Asp and Lys(**II**) (50 mM) or Arg(**I**) (50 mM) for either component when compared to solutions containing only one component. Furthermore, no coupled protons were found between the trisodium salt of Boc-Phe-Asp-Asp and Arg(**I**) or Lys(**II**) (50 mM of both components in $D_2O$) when examining NOESY spectra. The lack of binding between Boc-Phe-Asp-Asp and Arg(**I**) or Lys(**II**) shows that an aromatic ring needs to be positioned below a carboxylate to obtain binding in water.

Conjugate bases of carboxylic acids with higher p$K_a$'s will bind cationic ligands more tightly.[30] Therefore, a relative measure of carboxylate reactivity was sought by comparing the p$K_{a2}$ values of the templates (Table 2). The larger changes in p$K_{a2}$ found for the aromatic templates **1** and **2** in the presence of 0.05 M Arg(**I**) are consistent with salt bridge formation. The lack of association displayed by template **4** for Arg(**I**) or Lys(**II**) can be explained by its lower p$K_{a2}$. The p$K_{a2}$ of template **3**, however, is similar to the ones obtained for templates **1** and

(27) Springs, B.; Haake, P. *Bioorg. Chem.* **1977**, *6*, 181−190.
(28) (a) Schneider, H.-J.; Schiestel, T.; Zimmermann, P. *J. Am. Chem. Soc.* **1992**, *114*, 7698−7703. (b) Petti, M. A.; Shepodd, T. J.; Barrans, R. E.; Dougherty, D. A. *J. Am. Chem. Soc.* **1988**, *20*, 6825−6840.
(29) Gallivan, J. P.; Dougherty, D. A. *J. Am. Chem. Soc.* **2000**, *122*, 870−874.
(30) Chen, J. G.; McAllister, M. A.; Lee, J. K.; Houk, K. N. *J. Org. Chem.* **1998**, *63*, 4611−4619.

**2**, but **3** did not bind the amino acids. Thus, raising the p$K_a$ of a carboxylate does not guarantee salt bridge formation. p$K_a$ values of the templates were also measured in DMSO. Not surprisingly, their values are larger in DMSO than in water (data not shown), which is consistent with the larger binding constants observed in this solvent compared to those in water (Table 1). As seen in the aqueous studies, the size of p$K_{a2}$ was not correlated with the binding energies observed in DMSO-$d_6$.

A series of experiments were performed to determine if the observed binding energy originated from the aromatic ring, the carboxylates, or a combination of both functional groups. Individual contributions to association, e.g., salt bridge and cation$-\pi$ interactions, were assessed through potentiometric titrations. Addition of a salt to a carboxylic acid can result in a change of its p$K_a$ through ionic bond formation or by an increase in the ionic strength of the solution.[27] Association constants for salt bridges are derived by subtracting the drop in p$K_a$ due to the change in ionic strength from the overall change in p$K_a$. In our studies, $\Delta$p$K_{a2}$'s of the templates (derived by subtracting their p$K_{a2}$'s measured in 1 M KCl, 1 M guanidinium chloride ($GH^+$), or 0.05 M Arg(**I**) solutions from ones obtained in neat solutions) were approximately equivalent (Table 2), except for aromatic templates **1** and **2** in the presence of Arg(**I**), which were substantially larger. $\Delta$p$K_{a2}$'s were converted to free energies[27] to provide maximal energies for interactions between KCl, $GH^+$, or Arg(**I**) and the templates. The calculated $\Delta G°$'s are more favorable than those obtained from $^1$H NMR titrations (Table 1). Because the carboxylates of the templates in the NMR experiments had either $Na^+$ or $K^+$ as their couterions, it is possible that Arg(**I**) and Lys(**II**) have to compete with the $Na^+$ or $K^+$ for the binding site, which lowers their measured $K_A$'s. The same $K_A$'s were measured for solutions containing 2 equiv of $Na^+$ per template with and without the presence of 0.1 M potassium phosphate. This result suggests that contact ion pairs do not exist and the drops in p$K_{a2}$'s are caused by a change in the dielectric constants of the solutions. On the other hand, $\Delta$p$K_{a2}$ for template **4** is not consistent with the other templates, which could be a result of weaker association between template **4** and the cations. If $K^+$ and $GH^+$ form a salt bridge with the templates, the templates bind the cations equally, but weakly.

Because the drop in p$K_{a2}$'s of the aromatic templates is similar to that of the other templates in the presence of $K^+$ or $GH^+$, the cation$-\pi$ interaction[25,28,29] appears to be weak. Cation$-\pi$ interactions were not observed in $^1$H NMR assays when phenol was used as a model aromatic ring. No changes in the chemical shifts of Arg(**I**) or phenol were observed, except for a slight broadening of the phenolic proton, when these components were mixed (0.1 M for both Arg(**I**) and phenol). There was also no detectable change in phenol's p$K_a$ in a 50 mM solution of $GH^+$.

Important insight into the driving force for salt bridge formation with Arg(**I**) was obtained by examining changes in the first p$K_a$ of the dicarboxylates (data not shown). The p$K_{a1}$'s of templates **1**$-$**4** were reduced with the addition of $K^+$ and $GH^+$ in a manner similar to that for p$K_{a2}$. In the presence of Arg(**I**), however, large increases in p$K_{a1}$ were observed for templates **2** and **4** ($\Delta$p$K_{a1}$ = 1.1 and 0.8, respectively). p$K_{a1}$ for template **1** dropped in the presence of $K^+$ and $GH^+$ but remained approximately constant with Arg(**I**). A rise in p$K_a$ results from an unfavorable environment for ionization, such as placing a carboxylic acid near hydrophobic groups. Most likely for the SACA templates, the alkyl portion of arginine's side chain associates favorably with the aromatic rings of these templates prior to ionization and raises the p$K_{a1}$'s of their carboxylic acids. Once deprotonation occurs, the guanidinium moiety forms a salt bridge. This bridge is stabilized by the apolar environment caused by the aromatic ring and the alkyl side chain of Arg(**I**). The salt bridge promotes deprotonation of the second carboxylic acid, lowering p$K_{a2}$.

***Table 3.*** Maximum Solubility of the Templates and Their Ability To Transport Arg(I) from Water to 1-Octanol at 298 K

| template | $[template]_{max}$[a] (M) | $[Arg\cdot T]_{octanol}$[b]/$[Arg]_{octanol}$ |
|---|---|---|
| **1** | 0.137 ± 0.001 | 3.8 ± 0.2 |
| **2** | 0.011 ± 0.001 | 20.0 ± 0.3 |
| **3** | 0.03 ± 0.01 | 2.8 ± 0.2 |
| **4** | 0.17 ± 0.01 | 1.2 ± 0.2 |

[a] 0.1 M phosphate buffer at pH 7.5. [b] Transport efficiency is given by the ratio of the concentration of Arg(**I**) observed in 1-octanol with and without the presence of a template.

The existence of a potential SACA site in the interior of the $\alpha$-amylase protein[2b] suggests that it may be an important component of the protein folding process. We modeled this folding event by comparing the relative potential of the templates to transport Arg(**I**) from water (0.1 M phosphate pH 7.5) to 1-octanol (Table 3). 1-Octanol has a smaller dielectric constant than water, and it is commonly used to represent biological properties such as lipophilicity in the Log *P* coefficient[31] and the hydrophobic interior of proteins.[32] Because of a smaller desolvation penalty, salt bridge formation in 1-octanol is a more favorable process than that in water. Template **2** efficiently transports Arg(**I**) into 1-octanol, giving a 20-fold increase in its concentration. In the transport study of template **1**, a small amount of a salt containing template **1** and Arg(**I**) precipitated, which lowered its transport efficiency. Covering the charges with hydrophobic groups pays for a portion of the desolvation penalty, making immersion into a hydrophobic domain, such as a protein interior, more favorable.

## Discussion

Sites on protein surfaces that have charged groups combined with apolar groups in close proximity, such as in the SACA structure, may be sites that form stable salt bridges.[33] In simple terms, salt bridge formation is a spontaneous process if the energy gained by association of the ions and resolvation of the bridge[34] is larger than the energy lost though ion desolvation. The greater binding free energies observed in our studies for salt bridges in DMSO compared to those in water ($\delta\Delta G° = -1$ kcal/mol for Arg(**I**) and $\delta\Delta G° = -2.5$ kcal/mol for Lys(**II**), Table 1) are consistent with the larger desolvation penalty that occurs in water for these ions.

SACA templates provide binding specificity for the derivatized amino acids in DMSO but not in water. Whether the greater binding strength displayed by Lys(**II**) over Arg(**I**) when bound to the various templates in DMSO (on average $\delta\Delta G° =$

(31) (a) Buchwald, P.; Bodor, N. *Curr. Med. Chem.* **1998**, *5*, 353−380. (b) Hansch, C.; Leo, J. A. *Substituent Constants for Correlation Analysis in Chemistry and Biology*; John-Wiley and Sons: New York, 1979.
(32) (a) Chan, H. S.; Dill, K. A. *Annu. Rev. Biopharm. Biomed.* **1997**, *26*, 425−459. (b) Morton, A.; Baase, W. A.; Matthews, B. W. *Biochemistry* **1995**, *34*, 8564−8575.
(33) (a) Sheinerman, F. B.; Norel, R.; Honig, B. *Curr. Opin. Struct. Biol.* **2000**, *10*, 153−159. (b) Lo Conte, L.; Chothia, C.; Janin, J. *J. Mol. Biol.* **1999**, *285*, 2177−2198.

−1 kcal/mol) is a result of the difference in the solvation energy of the separated ions or of the complex or due to the difference in ionic bond strength depends greatly on the geometry of the complex.[34] If we assume that both side chains bind in a similar manner, Lys(**II**) forms a more stable complex because it forms an intrinsically stronger ionic bond than Arg(**I**). Lysine's cationic charge is shared with three N−H hydrogens instead of arginine's five. This greater charge distribution of arginine, however, gives it a smaller desolvation penalty when forming complexes in DMSO.

The binding free energies for the complexes between Lys(**II**) and Arg(**I**) with templates **1** and **2** in water were approximately equivalent. This lack of specificity for Arg(**I**) was surprising because previous studies have shown that phosphate forms a stronger salt bridge with guanidinium chloride than *n*-butylammonium chloride in water.[27] Association between *n*-butylammonium chloride and acetate is actually an unfavorable process. Our prediction that Arg(**I**) would form a more favorable complex also stemmed from our observation that the side chain of arginine was associated with a SACA structure and not lysine in the X-ray structures of protein binding domains that we examined.[2c,19,21,23] Furthermore, arginine is commonly found at protein binding interfaces with a 4-fold preference compared to the rest of the surface, whereas lysine is only twice as likely to be at the interface.[35] Using the solvation data provided by Langlet et al.[34] and assuming a similar binding geometry for both complexes, Arg(**I**) should be bound preferentially because the guanidinium side chain has a smaller desolvation penalty in water. Solvation of the salt bridge also favors Arg(**I**). The existence of apolar groups below the carboxylates, which block solvent molecules, reduces the importance of the resolvation term. Another important consideration is the entropic change that occurs upon complexation, which could be significant. On the other hand, there is the ever-present compensative nature between enthalpic and entropic values for processes that occur in water.[36] We are currently measuring the changes in enthalpy and entropy that occur upon salt bridge formation in our model system.

The large desolvation penalty experienced by small ions upon salt bridge formation is evident by the weak association observed between most of the cations and the templates (Table 2). Interactions between the aromatic templates and Arg(**I**) are substantial in water and unique among the templates (Tables 1 and 2). The aromatic rings of templates **1** and **2** provide for partial water desolvation of their carboxylates through the hydrophobic effect and by partially covering them. Mapping of water molecules in protein X-ray structures has shown that aromatic rings are preferentially solvated at their edges and avoid their face.[39] Accordingly, the aromatic face of a SACA site is readily desolvated. Having only a few water molecules at a highly electron rich center makes the SACA site unstable and, thus, more reactive toward cation binding.

Template **4**, which contains a leucine side chain below the diacids, should also promote salt bridge formation through partial water desolvation. According to $^1$H NMR titrations, a salt bridge does not exist between template **4** and Arg(**I**) in water. Results from potentiometric titrations, however, suggest that template **4** should weakly bind Arg(**I**). It should be noted that the binding energies derived from potentiometric titrations are consistently more negative than ones obtained from NMR titrations. Template **4** also had the smallest drop in p$K_{a2}$ in the presence of Arg(**I**), $K^+$, or $GH^+$ as compared to the other templates. We conclude that template **4** does not form a salt bridge in water. This lack of association shows that the placement of carboxylates in a hydrophobic environment does not guarantee favorable salt bridge formation.

One possible reason template **4** does not form a salt bridge with Arg(**I**) or Lys (**II**), whereas templates **1** and **2** do, is that the aliphatic portion of the amino acid side chain interacts more favorably with aromatic rings than with aliphatic groups. Strong associations between alkyl chains and aromatic rings have been observed in Wilcox's molecular torsional balance experiment[37] and in Monte Carlo simulations.[38] Potentiometric titrations showed that p$K_{a1}$ is raised for both templates **2** and **4**, which we attributed to association between the aliphatic portion of Arg(**I**) and the aromatic and aliphatic groups below the carboxylates, respectively. Another possible advantage aromatic rings have over aliphatic groups is their flat shape, which reduces the steric clashes and loss of entropy that occur upon association. It is possible that a stable complex geometry cannot be obtained for template **4** and Arg(**I**) or Lys(**II**).

Template **4** also has a substantially lower p$K_{a2}$ than do templates **1** and **2**, which suggests another source of free energy provided by the aromatic rings. The electron-rich aromatic faces of templates **1** and **2** raise the p$K_a$'s of their acids. Conjugate bases of carboxylic acids with larger p$K_a$'s are more reactive for ligand binding.[30] Enzymes can provide free energy to enhance the rates of chemical transformations by raising the p$K_a$'s of their side chains.[40] It is possible that protein binding domains use the same mechanism, but in these cases, it is used for ligand binding. The carboxylates have to be held at the face of an aromatic ring and in close proximity to be activated. Having an aromatic ring positioned next to the carboxylates is not sufficient for binding, as evident by the lack of association between Boc-Phe-Asp-Asp and Arg(**I**) or Lys(**II**) in water.

As discussed previously, a large p$K_a$ is not the sole criterion for salt bridge formation in water. Favorable interactions between the alkyl portion of Arg(**I**)'s side chain and a hydrophobic patch at a combining site is necessary besides an activated carboxylate. Thus, aromatic rings and carboxylates, in combination, on protein surfaces are likely sites for the initial association of a ligand's hydrophobic groups followed by desolvation and salt bridge formation.

The fact that template **2** binds the amino acids as well as template **1** was unexpected. Template **1** contains a phenolic ring that could potentially form an additional H-bond. Furthermore, phenolic rings are found preferentially at binding interfaces, and phenyl rings are not (Tyr and Phe are 3.0 and 0.5 more likely, respectively, to be at the binding interface than elsewhere on

(34) Langlet, J.; Gresh, N.; Giessnerprettre, C. A. *Biopolymers* **1995**, 36, 765−780.
(35) Bogan, A. A.; Thorn, K. S. *J. Mol. Biol.* **1998**, *280*, 1−9.
(36) (a) Lumry, R.; Ranjender, S. J. *Biopolymers* **1970**, *9*, 1125−1227. (b) Leffler, J. E. *J. Org. Chem.* **1955**, *20*, 1202−1231.
(37) (a) Kim, E.; Paliwal, S.; Wilcox, C. S. *J. Am. Chem. Soc.* **1998**, *120*, 11192−11193. (b) Nakamura, K.; Houk, K. N. *Org. Lett.* **1999**, *1*, 2049−2051.
(38) Jorgensen, W. L.; Severance, D. L. *J. Am. Chem. Soc.* **1990**, *112*, 4768−4774.
(39) (a) Hakansson, K. *Int. J. Biol. Macromol.* **1996**, *18*, 189 (b) Mitchell, J. B. O.; Nandi, C. L.; Thornton, J. M.; Price, S. L.; Singh, J.; Snarey, M. A. *J. Chem. Soc., Faraday Trans. 1* **1993**, *89*, 2619−2630.
(40) (a) Maranville, E.; Zhu, A. *Eur. J. Biochem.* **2000**, *267*, 1495−1501. (b) Fersht, A. *Enzyme Structure and Mechanism*, 2nd ed; W. H. Freeman and Co.: New York, 1985; Chapter 5.

the surface).[35] According to our results, however, phenyl rings should be as effective as phenolic rings for promoting salt bridge formation. One possible reason for the preference of Tyr at protein binding domains is the greater water solubility of its phenolic side chain. Template **1**, has a 10-fold greater solubility in water than that of template **2** (Table 3). Apparently, phenylalanine at a binding site would make it too apolar to exist on the surface exposed to the aqueous environment.

It seems that binding domains are finely tuned. The aromatic ring of Tyr (and we assume the same for Trp) in a SACA structure activates a carboxylate and provides for a hydrophobic patch that partially desolvates the carboxylate and binds to a hydrophobic patch of a ligand without being so hydrophobic that it would not be exposed on a protein's surface.

Salt bridges within proteins may benefit protein stability and have an important role in protein folding. Being directional, ionic bonds between side chains could help to establish the overall architecture of a protein's interior necessary to form a tightly packed hydrophobic core. Several factors, such as the desolvation cost of the ions and the flexibility of their side chains, determine whether salt bridge formation stabilizes a protein.[41] As stated previously, there is computational evidence that shows buried salt bridges can be energetically favorable. The strongest buried salt bridge, as determined by continuum electrostatic calculations, occurs between Glu27 and Arg387 of the human salivary α-amylase with a free energy value of −22.4 kcal/mol.[2b] Nussinov states that the precise geometry of this salt bridge is the key to the strong interactions, which overcomes its large desolvation penalty. We suggest that this penalty may actually be considerably smaller than calculated because this salt bridge is part of a SACA structure. The phenolic ring of Tyr31 is positioned below the carboxylate of Glu27 and the guanidinium moiety of Arg387 (Figure 1B).

Formation of SACA structures could be an energetically favorable step in the folding process of proteins. Being composed of only a few residues, the SACA structure could be a nucleation site in the nucleation condensation model.[42] Favorable salt bridge formation, moreover, is one possible method used by proteins to proceed to stage two of the two-state model of protein folding.[43] In the sequential collapse mechanism, desolvation is a key component for lowering the activation barrier of protein folding,[44] and desolvation may be one important component of SACA structures for salt bridge stabilization. We envisage that after the initiation of a protein's hydrophobic collapse, a carboxylate may be positioned over an aromatic face and available to interact with a lysine or arginine residue. Once the SACA structure has been established, protein folding continues, burying the salt bridge in a process that is more favorable than if bare charges were transferred from the aqueous milieu to the protein interior. This hypothesis is supported by the fact that SACA templates transport Arg(**I**) into 1-octanol to a greater extent than non-SACA templates (Table 3).

(41) Barril, X.; Aleman, C.; Orozco, M.; Luque, F. J. *Proteins* **1998**, *32*, 67−79.
(42) (a) Thirumalai, D.; Klimov, D. K. *Curr. Opin. Struct. Biol.* **1999**, *9*, 197−207. (b) Fersht, A. R. *Curr. Opin. Struct. Biol.* **1997**, *7*, 3−7.
(43) Arai, M. Kuwajima, K. *Adv. Protein Chem.* **2000**, *53*, 209−282 and references therein.
(44) Bergasa-Caceres, F.; Ronneberg, T. A.; Rabitz, H. A. *J. Phys. Chem. B* **1999**, *103*, 9749−9758.

## Conclusion

Our search for a model site of protein binding domains has led to the investigation of SACA sites found at binding domains of various proteins and within them as well. The carboxylates and aromatic ring were both necessary to bind Arg(**I**) and Lys(**II**) in water. The acidity constant of a carboxylic acid is increased when it is placed within van der Waals distance of an aromatic face, and once deprotonated, the carboxylate binds positively charged amino acids. We were surprised to find that templates containing aliphatic groups and carboxylates did not form salt bridges in water. It seems that the hydrophobic patches of the SACA sites and the amino acids associate initially. This preassociation of hydrophobic patches would undoubtedly increase the overall hydrophobicity of the combining site, decrease the desolvation penalty, and increase the strength of a salt bridge. Without ionic bond formation, the fleeting hydrophobic contact would break and the ligand would move onward, searching for a new site or being lost to the bulk solvent.

## Experimental Section

Solvents, reagents, and starting materials for the templates were purchased from Aldrich. The derivatized amino acids are available commercially (Lys(**II**) from Sigma and Arg(**I**) from CHEM-IMPEX). Asp-Asp and Boc-Phe were obtained from Sigma and Peptide International, respectively. $^1$H NMR and $^{13}$C NMR spectra were obtained from a Bruker 250 MHz NMR spectrometer. Two-dimensional $^1$H NMR spectra were obtained using a 400 MHz Bruker spectrometer. A MEL-TEMP (Laboratory Devices) apparatus was used to determine the melting points of the compounds; these values are given uncorrected. HPLC analysis was performed on a Shimadzu 10A series HPLC. UV−vis titrations were performed on a Hewlett-Packard Kayak XA series spectrophotometer. Solvents were purified by drying over a suitable drying agent and then distilled. Water for potentiometric titrations and HPLC assays was purified on a Millipore water purification system.

**Syntheses.** Templates **2** and **3** were synthesized through Diels−Alder reactions between maleic anhydride and anthracene or cyclohexadiene, respectively, followed by anhydride hydrolysis, according to literature procedures.[45,46] The properties of the templates matched those reported in the literature (for **2**, mp 264 °C,[45] found 266 °C; for template **3**, mp 152 °C,[27] found 148−150 °C). The route used to synthesize template **4** is given in Scheme 1.

***cis*-9,10-Dihydroanthracene-2,6-dihydroxy-9,10-*endo*-α,*β*-succinic Acid (1).** TMS-protected 2,6-dihydroxyanthracene[28b] (0.25 g, 0.72 mmol) and maleic anhydride (0.071 g, 0.72 mmol) were refluxed in 3 mL of freshly distilled dioxane for 16 h under Ar. After the solution was cooled, 0.5 mL of a 2 M $Na_2CO_3$ solution was added, and the solution was refluxed for 1 h. The impure product was extracted with 1 N HCl/EtOAC. The aqueous phases were collected, and the solvent was removed in vacuo. Template **1** was purified on silica using $CH_3CN/CH_3CO_2H$ (97:3) as the eluent to give 0.21 g (0.64 mmol, 89%) of product as a colorless glass. TOF MS: $m/z$ $MNa^+$ ($C_{18}H_{14}O_6Na$) calcd 349.0712, obsd 349.0742. $^1$H NMR (DMSO-$d_6$): $\delta$ 9.48 ppm (2H, bs), 7.19 ppm (1H, d, $J$ = 7.5 Hz), 7.06 ppm (1H, d, $J$ = 7.3 Hz), 6.86 ppm (1H, s), 6.69 ppm (1H, s), 6.53 ppm (2H, m), 4.60 ppm (2H, s), 2.50 ppm (2H, s). $^{13}$C NMR (DMSO-$d_6$): $\delta$ 171.7, 171.6, 156.2, 156.0, 143.0, 131.1, 129.0, 125.5, 125.0, 112.9, 112.2, 112.1, 111.8, 48.4, 48.2, 43.9.

**5,6-Dihydroxybicyclo[2.2.1]heptane-2,3-dicarboxylic Acid Dimethyl Ester (6).** A 100 mL round-bottom flask was charged with 3.5

(45) Weber, E.; Csõregh, I.; Ahrendt, J.; Finge, S.; Czugler, M. *J. Org. Chem.* **1988**, *53*, 5831−5839.
(46) (a) Bergmann, E. D.; Shahak, I. *J. Chem. Soc.* **1959**, 1418−1422. (b) Alder, K.; Stein, G. *Justus Liebigs Ann. Chem.* **1933**, *504*, 224−257.

*Scheme 1*

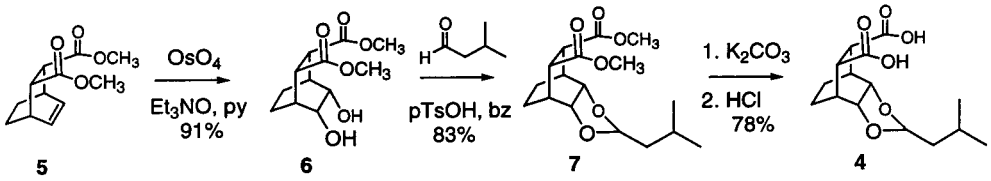


g (0.020 mol) of dimethyl ester 5,[46] 30 mL of *tert*-butyl alcohol, 8 mL of $H_2O$, and 1.3 mL of pyridine. After the diester dissolved, 2.5 g (0.022 mol) of triethylamine oxide was added followed by ca. 5 mg of OsO4 in *tert*-butyl alcohol. The reaction was refluxed for 20 h, and the solution turned brown. After the solution was cooled, 8 mL of 20% $NaHSO_3$ was added, and the majority of the *tert*-butyl alcohol was removed in vacuo. NaCl was added to saturate the aqueous phase, and the material was extracted with $Et_2O$. The organic layers were collected and dried with $MgSO_4$, and the solvent was removed in vacuo. The crude material was separated via column chromatography on silica using $CHCl_3$/MeOH (95:5) as the eluent to yield 3.8 g (15 mmol, 91%) of the desired product as a waxy solid. TOF MS: *m*/*z* $MNa^+$ ($C_{16}H_{24}O_6Na$) calcd 335.1448, obsd 335.1471. $^1$H NMR ($CDCl_3$): $\delta$ 3.98 ppm (2H, s), 3.58 ppm (2H, m), 3.52 ppm (6H, s), 2.88 ppm (2H, s), 2.11 ppm (2H, s), 1.90 ppm (2H, d, $J$ = 7.5 Hz), 1.12 ppm (2H, d, $J$ = 7.5 Hz). $^{13}$C NMR ($CDCl_3$): $\delta$ 173.5, 64.2, 51.7, 43.2, 33.7, 18.2.

**4-Isobutyl-3,5-dioxatricyclo[5.2.2.0]undecane-8,9-dicarboxylic Acid Dimethyl Ester (7).** A 25 mL round-bottom flask was dried and charged with 0.40 g (1.5 mmol) of diol template **6**, 0.20 mL (1.9 mmol) of isovaleraldehyde, ca. 10 mg of pTsOH, and 10 mL of benzene freshly distilled over $CaH_2$. The reaction was refluxed for 8 h under Ar. Solvent was removed in vacuo, the crude material was extracted with $H_2O$/$CH_2Cl_2$, and the organic layers were collected and dried over $MgSO_4$. After the solvent volume was reduced, the crude material was purified via column chromatography using $CH_2Cl_2$/MeOH (97:3) as the eluent. A 0.41 g amount (1.2 mmol, 83%) of diol template **7** was obtained as a yellow oil. TOF MS: *m*/*z* $MNa^+$ ($C_{17}H_{26}O_6Na$) calcd 349.1627, obsd 349.1598**.** $^1$H NMR ($CDCl_3$): $\delta$ 4.84 ppm (1H, t, $J$ = 5 Hz), 4.22 ppm (2H, s), 3.71 ppm (1H, m), 3.64 ppm (6H, s), 3.07 ppm (2H, s), 2.39 ppm (2H, s), 1.96 ppm (2H, d, $J$ = 8.0 Hz), 1.84 ppm (1H, m), 1.61 ppm (2H, m), 1.20 ppm (2H, d, $J$ = 8.0 Hz), 0.95 ppm (6H, d, $J$ = 6.2 Hz). $^{13}$C NMR ($CDCl_3$): $\delta$ 172.7, 102.0, 72.3, 51.5, 42.7, 41.8, 31.0, 24.4, 22.7, 18.1.

**4-Isobutyl-3,5-dioxatricyclo[5.2.2.0]undecane-8,9-dicarboxylic Acid (4).** A 25 mL round-bottom flask was charged with 0.40 g (1.2 mmol) of template **7** and 5 mL of a 2 M $K_2CO_3$/EtOH (50:50) solution. The reaction was refluxed for 10 h. After the solvent was removed under vacuum, the material was extracted with 1 M $Na_2CO_3$/$CH_2Cl_2$. The aqueous phase was collected, acidified with 1 N HCl, and then extracted with $Et_2O$. Organic phases were collected and dried with $MgSO_4$, which was subsequently filtered off. After the volume of $Et_2O$ was reduced, petroleum ether was added, and template **4** precipitated, yielding 0.28 g (0.94 mmol, 78%) of a white solid (mp 95−96 °C). TOF MS: *m*/*z* $MNa^+$ ($C_{15}H_{22}O_6Na$) calcd 321.1314, obsd 321.1299. $^1$H NMR (DMSO-$d_6$): $\delta$ 12.60 ppm (2H, s), 4.85 ppm (1H, t, 5 Hz), 3.99 ppm (1H, d, 6.2 Hz), 3.83 ppm (1H, d, 6.2 Hz), 3.02 ppm (1H, d, 6.5 Hz), 2.78 ppm (1H, d, 6.5 Hz), 2.23 ppm (2H, bd, $J$ = 8.8 Hz), 1.76 ppm (2H, m), 1.59 ppm (1H, m), 1.52 ppm (2H, m), 1.15 ppm (2H, m), 0.91 ppm (6H, d, $J$ = 6.5 Hz). $^{13}$C NMR (DMSO-$d_6$): $\delta$ 175.1, 174.9, 102.4, 75.1, 72.7, 41.9, 41.4, 32.0, 31.7, 24.4, 23.0, 17.8, 14.1.

**Boc-Phe-Asp-Asp.** A 25 mL round-bottom flask was dried and charged with 110 mg of Boc-Phe (0.40 mmol), 0.080 g of EDC (0.40 mmol), and 5 mL of DMF (distilled over $MgSO_4$ under vacuum). The reaction was left stirring under Ar at room temperature for 1 h. To this solution were added 0.10 g of Asp-Asp (0.40 mmol) and a catalytic amount of 1-hydroxybenzotriazole (HOBT). The reaction was sonicated overnight under Ar at room temperature. Purification on a $C_{18}$-loaded reversed-phase column using 0.1% TFA $H_2O$/$CH_3CN$ as the eluent resulted in 0.14 g (0.28 mmol, 70%) of Boc-Phe-Asp-Asp as a colorless oil. TOF MS: *m*/*z* $MH^+$ ($C_{22}H_{29}N_3O_{10}$) calcd 496.1931, obsd 496.1862. $^1$H NMR (mixture of conformers) ($D_2O$): $\delta$ 7.22−7.39 ppm (5H, m), 4.62 ppm (1H, bt, $J$ = 5.2 Hz), 4.45 ppm (1H, dd, $J$ = 8.1 Hz and $J$ = 5.0 Hz), 4.30−4.42 ppm (1H, m), 3.15−3.30 ppm (2H, m), 3.04 ppm (1H, bq, $J$ = 6.5 Hz), 2.96−2.90 ppm (2H, m) 2.84 ppm (3H, bs), 1.79 ppm (1H, bq, $J$ = 7.0 Hz), 1.34 ppm (6H, s). $^{13}$C NMR (DMSO-$d_6$): $\delta$ 174.7, 172.2, 171.7, 170.5, 159.1, 158.5, 155.6, 155.3, 154.5, 138.3, 137.8, 129.3, 128.1, 126.4, 126.2, 78.3, 78.1, 55.2, 54.3, 49.4, 48.7, 42.2, 41.2, 37.4, 37.1, 36.2, 36.0, 35.2, 28.1, 27.8.

**Potentiometric Titrations.** Generally, 20 mM template solutions were made with boiled, purified water (Millipore) containing 0.1 M KCl, 1 M KCl, 1 M guanidine hydrochloride, 0.05 M Arg(I), or no additional salt except for template **2**. Because of its poor solubility at low pH, template **2** was analyzed as a 1 mM solution. Potentiometric titrations were performed by adding aliquots of a 0.845 N NaOH solution. For titrations in DMSO, the electrode was calibrated using standard solutions of 2,6-dinitrophenol and 4-chloro-2,6-dinitrophenol, according to literature procedures.[48] Five millimolar solutions of the templates were prepared in freshly distilled DMSO (over $CaH_2$) and titrated with a 0.10 M solution of $Bu_4NOH$ in DMSO. The p$K_a$ values of the templates were calculated using the BEST program.[49]

**Transport and Solubility Studies.** Transport studies involved making 20 mM solutions composed of templates **1**−**4** and 50 mM Arg-(**I**) in phosphate buffer (100 mM pH 7.5). After an equal volume of 1-octanol was added, the solutions were vigorously stirred for 24 h at room temperature. To determine the concentrations of the components, aliquots from the 1-octanol layers were removed and then injected onto an HPLC $C_{18}$-bonded reversed-phase column, and their peaks were integrated. The integral values were converted to concentrations using correlation coefficients obtained from calibration curves constructed by plotting peak areas versus known concentrations of pure components. Maximal concentrations of templates **1**−**4** in 100 mM phosphate buffer pH 7.5 (Table 3) were obtained by briefly sonicating solutions that contained an excess amount of template and then vigorously stirring them for 24 h. The solutions were filtered followed by centrifugation at 10 000 rpm for 30 min, and the concentrations of the templates were determined by HPLC analysis for template **3** vide supra, by gravimetric analysis for template **4**, and by performing UV titrations for templates **1** and **2**. Extinction coefficients were derived for templates **1** and **2** by constructing calibration curves ($\lambda_{max}$ = 286 nm, $\epsilon = (3.1 \pm 0.1) \times 10^3$ and $\lambda_{max}$ = 273 nm, $\epsilon = (1.5 \pm 0.1) \times 10^3$, respectively). Standard deviations for these results were obtained by averaging values obtained from duplicate experiments.

**Monitoring Association.** Association of these templates and Boc-Phe-Asp-Asp with Arg(**I**) or Lys(**II**) was monitored by $^1$H NMR titration studies in DMSO-$d_6$, $D_2O$, and buffered solutions (90/10 0.1 M phosphate buffer pH 7.5/$D_2O$) at 25.0 °C. Equilibrium constants were derived from plots of the changes in the chemical shifts of the α-H and δ-H protons for Arg(**I**) and α-H and ϵ-H protons for Lys(**II**) that occur with the increasing concentration of the template against the concentration of the template. A nonlinear least-squares fitting

(47) Williamson, K. L.; Hasan, M. U.; Clutter, D. R. *J. Magn. Reson.* **1978**, *30*, 367−383.
(48) Kolthoff, I. M.; Chantooni, M. K., Jr.; Bhowmik, S. *J. Am. Chem. Soc.* **1968**, *90*, 23−28.
(49) Martell, A. E.; Motekaitis, R. J. *The determination and use of stability constants*; VCH: New York, 1988.

procedure was used to solve eq 1, where the difference in the chemical

$$\Delta\delta = \Delta\delta_{obs} - \Delta\delta_0 = \frac{K_A[T]\Delta\delta_{max}}{(1 + K_A[T])} \quad (1)$$

shift ($\Delta\delta$) of an amino acid proton in the presence of template ($\Delta\delta_{obs}$) and in its absence ($\Delta\delta_0$) depends on the concentration of the template ([T]), the chemical shift of the proton when it is completely bound to the template ($\Delta\delta_{max}$), and the association constant of this complex ($K_A$). Because of the large association constant, a Benesi−Hildebrand plot[50] was used to obtain an approximate $K_A$ value for the binding between Boc-Phe-Asp-Asp and Lys(**II**) in DMSO-$d_6$. Association between the templates and positively charged side chains was verified by performing potentiometric titrations in the presence of Arg(I). NOESY experiments were performed on aqueous samples containing Boc-Phe-Asp-Asp and the amino acids with mixing times of 150, 300, and 500 ms to corroborate results obtained from one-dimensional $^1$H NMR titrations.

**Acknowledgment.** The authors thank the University of Cincinnati for their generous funding of this project and professor Estel Sprague for giving us a version of his computer program that provides for nonlinear least-squares analysis.

**Supporting Information Available:** Table of p$K_a$ values for templates **1**−**3** in DMSO and representative $^1$H NMR spectra of binding titrations of templates **1** and **2** with Arg(**I**) in $D_2O$ (PDF). This material is available free of charge via the Internet at http://pubs.acs.org.

JA011973H

(50) Benesi, H. A.; Hildebrand, J. H. *J. Am. Chem. Soc.* **1949**, *71*, 2703.